The multifaceted roles of M_nL_{2n} cages in catalysis

Ashbridge, Z.; Reek, J.N.H.

DOI
10.1038/s44160-024-00606-5

Publication date
2024

Document Version
Final published version

Published in
Nature Synthesis

nature synthesis

Review article

https://doi.org/10.1038/s44160-024-00606-5

The multifaceted roles of M_nL_{2n} cages in catalysis

Received: 7 March 2024

Accepted: 14 June 2024

Published online: 24 July 2024

Check for updates

Zoe Ashbridge & Joost N. H. Reek

Metal–organic cages are versatile supramolecular architectures, fulfilling various distinct roles in the mediation of catalysed chemical reactions. M_nL_{2n} cages have become increasingly synthetically accessible in recent years, and their modular nature allows for precise tailoring for specific applications. Sophisticated M_nL_{2n} cages have now been deliberately designed to fulfil several roles, providing unique reactivity that begins to emulate the highly complex nature of enzyme active sites. Here we highlight the different functions played by M_nL_{2n} cages in the context of catalysed synthetic reactions: (1) protection of catalysts or substrates, (2) activation or preorganization of guests and (3) concentration enhancement of reactants or catalysts in confined space. We conclude by discussing future directions for the field, such as the potential to increase complexity further by developing stimuli-responsive, flexible or reduced-symmetry cages, ultimately progressing artificial cage catalysis towards the levels of catalytic control provided by biological host–guest architectures.

Artificial supramolecular hosts have long sought to emulate enzyme catalysis by harnessing interactions within substrate binding pockets to control the reaction rate and selectivity[1]. Host–guest catalysis may exploit conformational restriction, employ multivalent interactions to stabilize transition states, and shield a cavity from bulk conditions[2]. Despite this, routine synthetic chemistry generally overlooks the use of host–guest systems for catalysis[3]. However, increasing numbers of examples of catalytically relevant host–guest architectures are allowing the fundamental principles of supramolecular catalysis to be rationalized, promising new synthetic strategies based on the adoption of this versatile approach[4]. Although the most commonly ascribed roles of a host–guest catalyst are to bind a substrate, stabilize the transition state of a transformation, and release the product, there are several other roles supramolecular hosts may assume in catalysis. For example, the host–guest complexation of simple crown ethers has long been exploited in diverse catalytic roles such as phase transfer catalysis and substrate recognition, in addition to the more classical electrostatic activation[5,6].

The development of new supramolecular architectures for applications in catalysis is commonly motivated by the biomimicry of enzyme active sites[7], which can themselves be viewed as supramolecular cavities that perform catalysis. Enzyme catalysis is exquisite; however, the size and complexity of enzymes makes the rational design of artificial enzymes challenging[8]. Additionally, the application of enzymes is often limited to a narrow range of aqueous conditions. By contrast, artificial supramolecular host–guest catalysts can exploit greater structural diversity, expanding their catalytic application to a broader range of conditions and reactions. Metal–organic cages are particularly attractive candidates for host–guest catalysis due to their modularity, ease of self-assembly, relative component simplicity and control of size- and shape-specificity[9–12]. This enables the rational design of supramolecular cavities and offers the potential to introduce further complexity by variation of the metal nodes or addition of pendant functionality to the organic components[13].

This Review will focus on the use of M_nL_{2n} cages—in which the metal-to-ligand ratio is 1:2—in the context of catalysis. M_nL_{2n} cages are robust, can be reliably prepared from easily synthesized and readily functionalized ligands, and offer controllable modularity to exploit a wide range of cavity sizes and space[14]. The self-assembly behaviour of dipyridyl ligands with a variety of bend angles in the presence of square-planar Pd(II) or Pt(II) metal nodes has been comprehensively explored by both experimental and theoretical means for over a decade (Fig. 1a)[15,16].

The modular metal–organic self-assembly approach to M_nL_{2n} cage formation allows a family of structures with a wide variety of

Van't Hoff Institute for Molecular Sciences, University of Amsterdam, Amsterdam, The Netherlands. e-mail: z.ashbridge@uva.nl; j.n.h.reek@uva.nl

https://doi.org/10.1038/s44160-024-00606-5

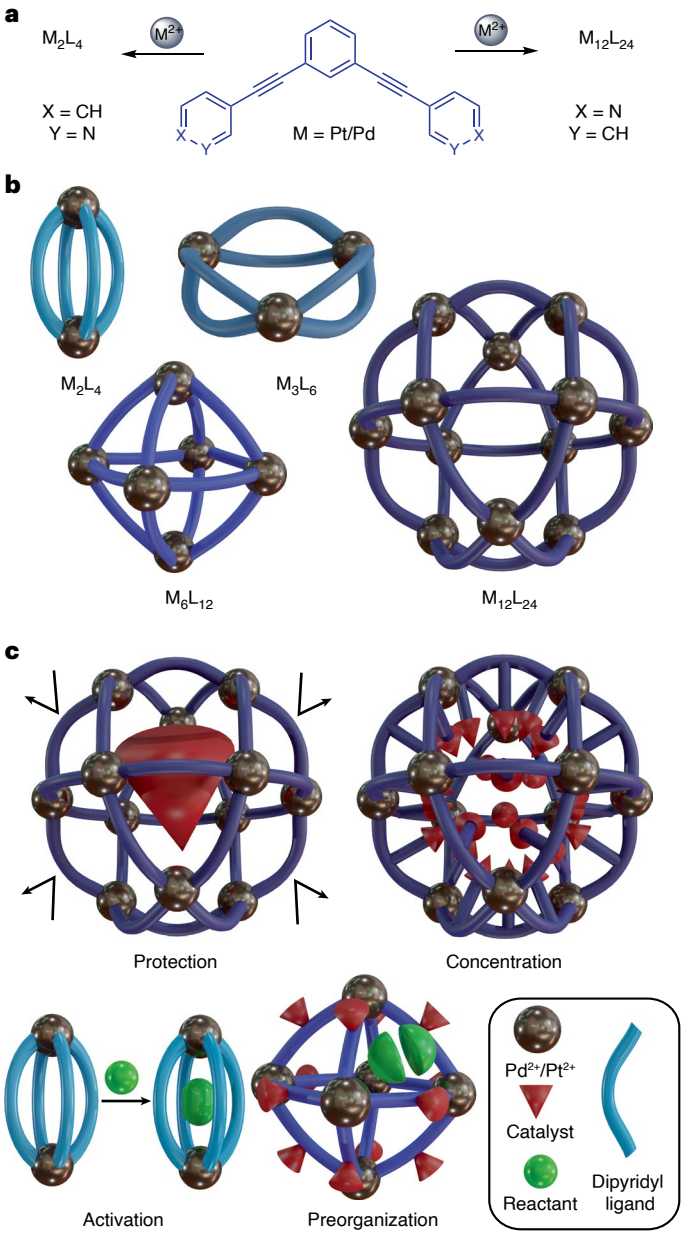

Fig. 1 | M_nL_{2n} cages and their roles in catalysis. a, Assembly of the two most common M_nL_{2n} architectures—M_2L_4 and $M_{12}L_{24}$—is controlled by positioning the substituent group (and therefore the orientation of the coordination vector) of a dipyridyl ligand at either the *meta* or *para* position, respectively. **b**, Cartoon depictions of the four types of M_nL_{2n} cage discussed in this Review: M_2L_4, M_3L_6, M_6L_{12} and $M_{12}L_{24}$. **c**, Examples of the four most common roles played by M_nL_{2n} cages: protection, concentration enhancement, activation and preorganization.

sizes and shapes to be generated from a library of simple and structurally similar ligands (Fig. 1b). M_2L_4 capsules (the smallest iterations of this class of cages) are generally barrel-shaped with a relatively small cavity size[17,18] capable of tightly binding counterions such as PF_6^- (ref. 19) or a single small organic molecule such as 1,4-benzoquinone[20]. Examples of M_3L_6 triangular architectures are less common[21,22], and often exist in dynamic equilibrium with alternative structures[23,24]. Other less frequently reported structures are M_4L_8 cages, which may describe either double-walled tetrahedra[25,26] or two interpenetrated M_2L_4 cages[27], and cubic M_6L_{12} cages[28]. More common are $M_{12}L_{24}$ spherical cages, first reported by Fujita and colleagues in 2004 and often referred to as nanospheres[29], which are large enough to bind small proteins[30]. Relatively large $M_{24}L_{48}$ cages with internal cavity diameters of over 4 nm have since been reported[31]. As the size and complexity of such structures increases, the self-assembly must be more carefully controlled to minimize the likelihood of obtaining undesired kinetically trapped species[32,33].

The structural features of cage architectures have the potential to induce catalytic activity in different ways. The most obvious of these is the use of the reactivity of the constituent components, such as a ligand or metal node. As the constituent components are an integral part of the cage structure, their action in catalysis may be limited. The cage itself can also become an active catalyst once formed from otherwise inactive components, as it can bind and stabilize species. Alternatively, catalytic sites may be covalently appended to the ligand backbone and lie either internally (*endo*-) or externally (*exo*-) to the cage scaffold. We focus on *endo*-functionalized cages in this Review, as they exhibit the effects of nano-confinement[34]. As the availability and structural understanding of M_nL_{2n} cages has grown substantially in recent years, their properties can now be selected to functionally address specific challenges when designing and optimizing a chemical reaction[33].

Four key roles of M_nL_{2n} cages in catalysed reactions have been identified and will be discussed here: the protection of guests, the enhancement of local concentrations, and the activation and preorganization of substrates (Fig. 1c). In each case, the effect of the cage may be displayed in the context of reactants, products, catalysts or cofactors. The interplay between the roles is highlighted with selected examples displaying multiple roles. Finally, future directions of the field are discussed, with particular focus on the need to increase the structural complexity of M_nL_{2n} cages. There are now several examples of M_nL_{2n} cages fulfilling multiple complex roles in catalysed reactions, and therefore a review focusing on the varied roles of such architectures is timely.

Cages for catalyst protection

Metal–organic cages can be used for compartmentalization, creating isolated micro-environments within a bulk solution. The application of such (supra)molecular compartments for protection of an encapsulated species is a well-established theme in host–guest chemistry, introduced by Cram's 'taming of cyclobutadiene' over three decades ago[35]. By isolating a single reactive cyclobutadiene molecule within an organic cage, its otherwise rapid dimerization could be prevented[36]. The cyclobutadiene cannot escape from the cavity at room temperature and so is prevented from dimerizing in the bulk chloroform solution. Thus, a cage cavity with sufficient size to bind one guest but not two can effectively protect a compound from reacting with itself.

There are several other means by which a cage may provide protection to either a reactant or a catalyst. In addition to protecting a substrate from itself, two different species in solution may be protected from each other. By isolating two reactive species in separate cage architectures, prevention of their undesired interaction can allow cascade reactions to be achieved in one pot that are otherwise incompatible in the bulk solution. As an alternative structural approach to the non-covalent encapsulation of a guest, a metal–organic cage may instead incorporate covalently appended functional groups endohedrally (that is, pointing inside the cage) within its rigid ligand building blocks, thus ensuring that the vulnerable functionalities point inwards. In an elegant example of this by Fujita and colleagues, two different $Pd_{12}L_{24}$ nanospheres bearing either (2,2,6,6-tetramethylpiperidin-1-yl) oxyl (TEMPO) (**L1**) or MacMillan's catalyst (**L2**), respectively, as endohedrally functionalized ligands can be mixed in solution (Fig. 2a)[37]. A one-pot cascade reaction in which substrate **1** is first oxidized by Pd_{12}**L1**$_{24}$ to **2** and then cyclized by Pd_{12}**L2**$_{24}$ to **3** may then be performed. In contrast, when the two catalyst ligands are mixed in bulk solution, the TEMPO catalyst **L1** rapidly oxidizes the MacMillan catalyst **L2** and thus deactivates it, preventing the formation of product **3**. The site-isolation strategy of protecting a chosen catalyst endohedrally within a $Pd_{12}L_{24}$ nanosphere exploits the modularity and ease

https://doi.org/10.1038/s44160-024-00606-5

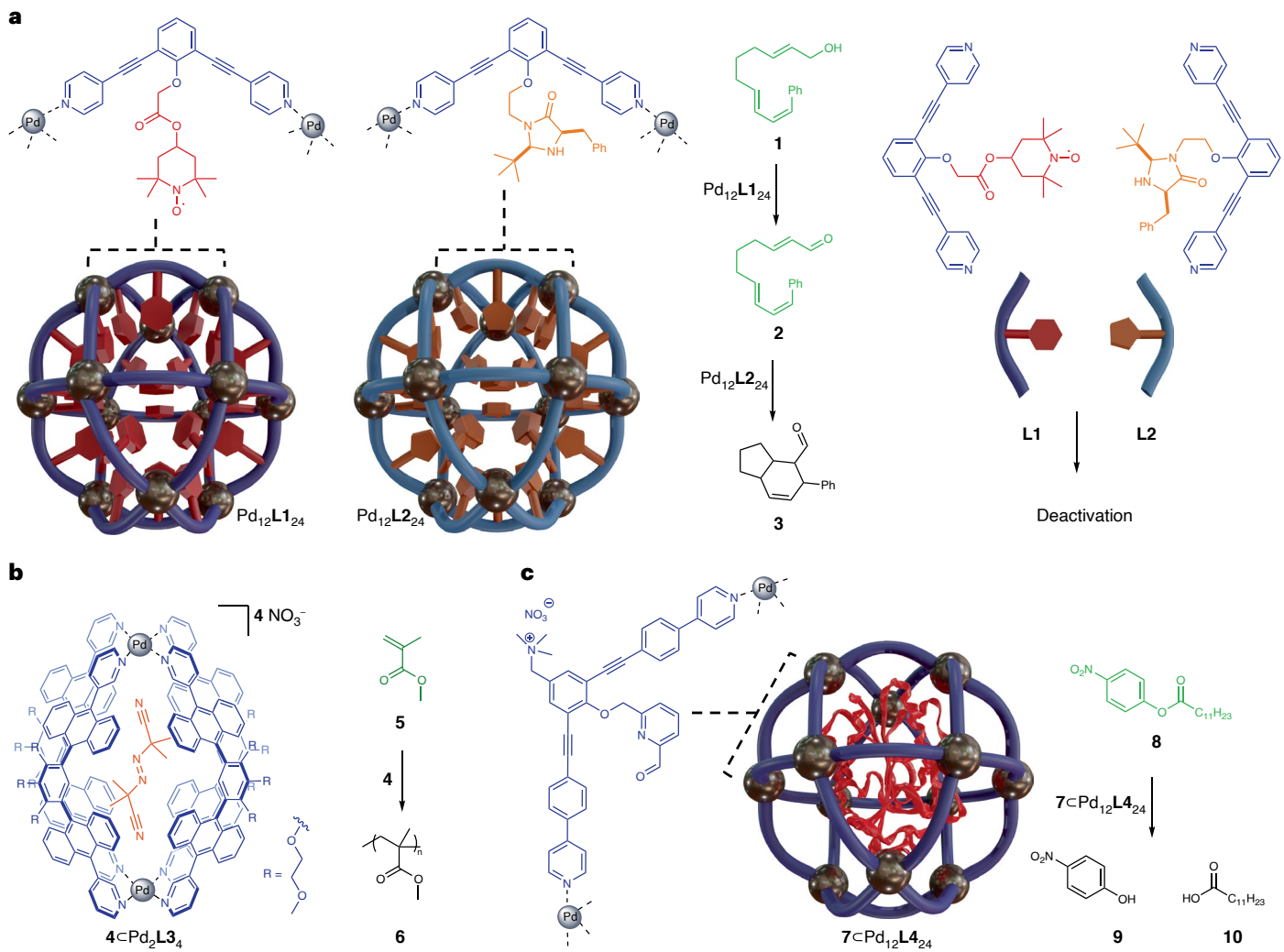

Fig. 2 | M_nL_{2n} cages for catalyst protection. a, Two different pre-formed nanospheres, $Pd_{12}L1_{24}$ and $Pd_{12}L2_{24}$, are applied as catalysts in the same reaction mixture[37]. Substrate **1** can be oxidized to **2** by $Pd_{12}L1_{24}$, followed by cyclization to **3** by $Pd_{12}L2_{24}$, in a one-pot cascade process. In contrast, mixing of ligands **L1** and **L2** in the same reaction mixture without the spatial protection afforded by the nanosphere leads to catalyst deactivation. **b**, Encapsulation of **4** in cage Pd_2L3_4 protects it from degradation by light and temperature[41]. Encapsulated **4** can be released on demand by changing the solvent to initiate, for example, polymerization of **5** to **6**. **c**, A cutinise-like enzyme **7**, which catalyses the hydrolysis of **8** to give **9** and **10**, is protected from degradation by encapsulation in cage $Pd_{12}L4_{24}$[44]. Ligands are shown in shades of blue, Pd^{2+} nodes as grey spheres, catalysts and initiators in red or orange, reactants in green and products in black.

of preparation of functionalized M_nL_{2n} structures, paving the way for more efficient and rapid one-pot multi-step syntheses.

In a demonstration of the increasing number of applications of such architectures, Johnson and colleagues have recently demonstrated that $Pd_{12}L_{24}$ cages with endohedrally bound TEMPO or AuCl catalysts may also be incorporated into polymer gels, facilitating heterogeneous catalysis while also protecting the internally bound catalytic sites[38]. Chen and colleagues have also confined a similar TEMPO-containing $Pd_{12}L_{24}$ cage architecture within mesoporous carbon for heterogeneous catalytic applications[39].

In addition to protection from other substrates, an encapsulated guest may require protection from specific reaction conditions (such as solvent, pH, light or temperature) that would otherwise lead to degradation. This application is particularly pertinent for compounds with notoriously poor stability, such as radical initiators[40]. Yoshiwaza and colleagues synthesized a Pd_2L_4 cage from ligand **L3**, incorporating light-absorbing anthracene panels. This was found to bind 2,2′-azobisisobutyronitrile **4** and related radical initiators (Fig. 2b)[41]. Under UV-light irradiation or increased temperature, the cage was effective in protecting the guest initiator and thus increasing its stability by ~600 times compared to the non-encapsulated substrate **4**. The variation in binding strength of the host–guest complex could then be exploited to release the protected guest **4** by changing from a polar solvent such as water to an apolar solvent such as toluene, initiating radical polymerization of methyl methacrylate **5** to poly(methyl methacrylate) **6** on demand. The cage therefore acts as a delivery vessel for an unstable substrate, as has also been demonstrated previously for tetrahedral metal–organic cages[42].

In a more structurally elaborate example, Clever and colleagues reported a Pd_4L_8 interpenetrated double cage incorporating ligands that act as singlet oxygen generators. The cage architecture successfully protects the photosensitizer ligand from degradation when exposed to the light irradiation required for the desired [2 + 4] hetero-Diels–Alder reaction[43].

Enzymes have well-known stability limitations, and these may also be protected from degradation by encapsulation. The modular nature of M_nL_{2n} cages readily allows for the construction of large internal compartments capable of binding small proteins[30]. For example, the stability of a cutinase-like enzyme **7** is markedly improved when it is bound as a guest within a $Pd_{12}L4_{24}$ cage (Fig. 2c)[44]. The endohedral formylpyridine

https://doi.org/10.1038/s44160-024-00606-5

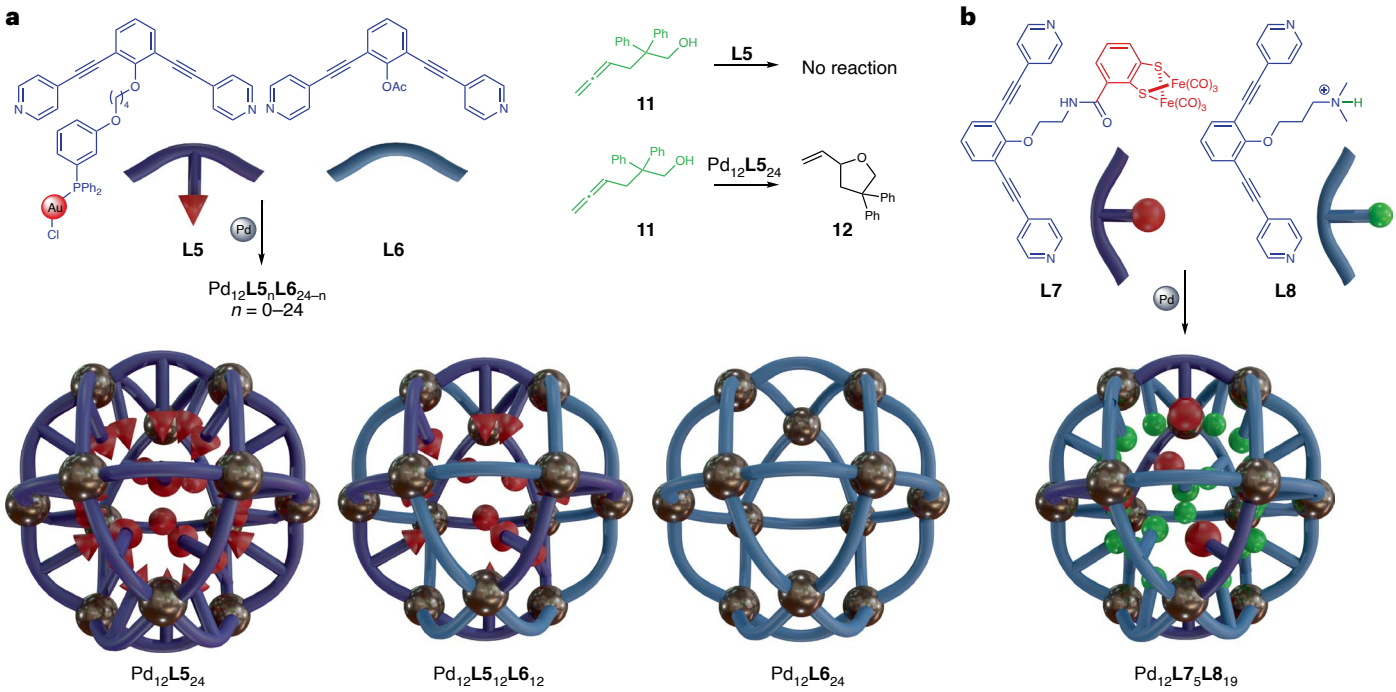

Fig. 3 | $M_{12}L_{24}$ cages for concentration enhancement. a, Changing the ratio of ligands **L5** and **L6** as components of an $M_{12}L_{24}$ cage changes the relative concentration of the AuCl complex from 0.05 M to 1.1 M (ref. 47). Sufficiently high local concentrations of AuCl within Pd_{12}**L5**$_{24}$ catalyses the cyclization of **11** to **12**. **b**, The concentration of both [FeFe] hydrogenase catalyst ligand **L7** and proton substrate-bearing ligand **L8** can be enhanced in the same cage architecture[51]. Ligands are shown in shades of blue, Pd^{2+} nodes as grey spheres, catalysts in red, reactants in green and products in black.

group of **L4** is required to form the nanosphere around guest **7** through reversible condensation with its terminal amine. Enzyme **7** catalyses the hydrolysis of ester **8** to give nitrophenol **9** and carboxylic acid **10**. Its active half-life in the presence of denaturing solvent was increased by three orders of magnitude when encapsulated, compared to uncaged **7**. By spatially isolating the enzyme within the cavity, it can refold after denaturing, without bulk aggregation. Because the size constraints of the nanosphere allow for binding of only one enzyme per cage, this effect is akin to markedly reducing the local concentration of enzyme in solution.

Cages for concentration enhancement

One of the most important features of cage architectures is the ability to generate conditions inside the cage that are different from the bulk. The local concentration of reactants or catalysts can be increased with respect to the bulk concentration by their encapsulation in supramolecular cages. As the concentrations of substrates and catalysts often appear in the rate equation, positive effects in catalysis can therefore be anticipated. This feature of self-assembled capsules has been known and exploited for decades. In an early example, the classic 'softball' organic capsules of Rebek were effective in binding a diene and a dienophile in close local proximity to increase the rate of Diels–Alder reactions[45]. However, substantial product inhibition was reported, as the product was bound more strongly than the substrate. This is a recurring issue in cage catalysis when a cage is used as a template for a fusion reaction, as the product binding is more entropically favourable than the binding of two substrates[12,46]. Catalysis with cages in which not only the preorganization of substrates leads to conversion, but the reaction is catalysed by an active (metal) site that resides in the cage, for example, typically shows fewer product inhibition issues[12].

A different synthetic approach that capitalizes on concentration effects is the application of larger cages that can host multiple catalysts and substrates, thereby emulating a small reaction vessel. Using this strategy, reactions can be performed at high local catalyst concentration, high local substrate concentration or a combination thereof. Large $M_{12}L_{24}$ cages may therefore be used as 'nano-concentrators' to bind multiple catalyst species and increase the local catalyst concentration within the cage. For example, Reek and colleagues have developed ligand **L5** bearing a Au(I) catalyst (Fig. 3a)[47]. When incorporated into a $Pd_{12}L_{24}$ cage in a varying ratio with respect to unfunctionalized ligand **L6**, local gold concentrations within the cage can be tuned from effectively 0.05 M to 1.1 M, while the overall concentration in the bulk is submillimolar. A complete lack of catalytic activity for the cyclization of allenol **11** at 0.05 M concentration is contrasted with the formation of desired product **12** in 90% yield after 12 h at 1.1 M local concentration. The very high local concentrations within the nanosphere are the primary reason for the increased catalytic activity, as evidenced by the lack of reaction when the same overall concentration of ligand **L5** is employed in bulk solution. New bands in the UV–vis spectrum suggest that multinuclear gold complexes form within the cage, and these act as the reactive species. The need for chloride abstraction—usually a prerequisite for catalysis using AuCl species—can be avoided by the extreme local catalyst concentrations employed in this study. By focusing the catalytic activity within the nanospheres in this manner, a low overall amount of gold catalyst is required for significant activity. In an extension to this work, the use of more kinetically stable Pt(II) nodes in related $Pt_{12}L_{24}$ nanospheres allows for a much greater range of Au-catalysed cyclization reactions under these conditions[48].

Reactions that proceed through dinuclear mechanisms typically display rate equations that are higher order in catalyst concentration (second order), and such reactions are anticipated to particularly benefit from high local catalyst concentrations, provided that there is enough flexibility to reach the required dinuclear intermediate. For this reason, specific $M_{12}L_{24}$ cages have been developed that can bind catalysts based on complementary hydrogen-bond interactions. For example, the copper(I)-catalysed cyclization of alkynoic acids proceeds via a bis-Cu(I) intermediate as the rate-determining step[49].

https://doi.org/10.1038/s44160-024-00606-5

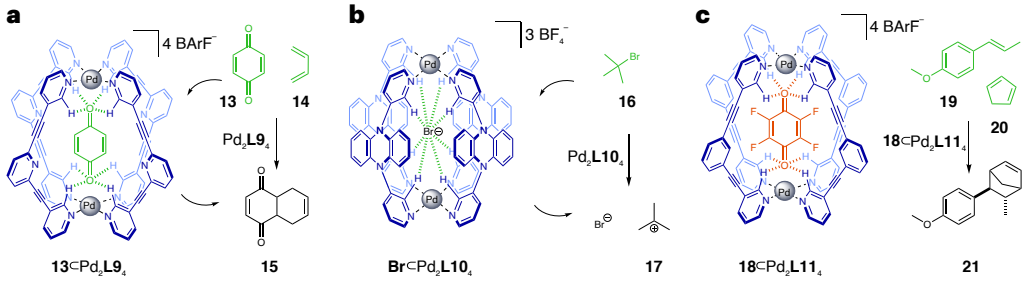

Fig. 4 | M_2L_4 cages for substrate activation. a, Dienophile **13** is electronically activated by encapsulation in Pd_2**L9**$_4$ to form Diels–Alder product **15** with diene **14**[56]. **b**, The alkyl halide bond of **16** is electronically activated for cleavage by encapsulation in Pd_2**L10**$_4$, to give Br^- and carbocation product **17**[60]. **c**, Encapsulation of quinone cofactor **18** within a cage Pd_2**L11**$_4$ enhances its oxidative properties, promoting the Diels–Alder reaction of **19** and **20** to form **21**[63]. Ligands are shown in shades of blue, Pd^{2+} nodes as grey spheres, cofactors in orange, reactants in green and products in black.

Concentrating Cu(I) catalysts within a $Pt_{12}L_{24}$ cage results in higher reaction rates, in line with the rate-determining dinuclear step, although there is also an element of substrate–catalyst preorganization. In a different example, the rate of electrochemical water oxidation catalysis by a Ru(IV) catalyst was demonstrated to be enhanced by a factor of 140 by only changing the local concentration of the Ru(IV) complexes within a $Pt_{12}L_{24}$ cage[50].

In a further example, which displays concentration enhancement of both catalyst and reactant, ligand **L7**, bearing a synthetic [FeFe] hydrogenase mimic, is incorporated into a $Pd_{12}L_{24}$ nanosphere alongside ligand **L8** bearing an ammonium salt (Fig. 3b)[51]. The catalytic overpotential is reduced as a result of binding within the nanosphere, leading to a high local concentration of catalyst in the vicinity of the positive cage framework, which probably stabilizes reduced intermediates. The high concentration of protons within the nanosphere due to significant **L8** incorporation outweighs the repulsion between the cationic cage and protons in the bulk solution, and the high local concentration of substrate (protons) ensures that the reaction rate remains high. In addition, controlled generation of a proton-rich environment around a hydrogenase catalyst mimics the presence of positively charged amino-acid residues around the active site of the naturally occurring hydrogenase enzymes[52].

Cages for activation

An important characteristic of metal–organic cages, especially when compared to their purely organic counterparts, is the often significant difference in electronic character between the centre of the cavity and the bulk solution, induced by the charged metal nodes. By exploiting this feature, coulombic binding and activation of reactants or catalysts can be achieved. This electronic activation of guests is one of the most employed roles of metal–organic cages in catalysis. Substrate activation by tetrahedral M_4L_6 cages for catalytic reactions is very well-established, with several examples reported by Nitschke[53], Raymond[54] and colleagues, among others.

For M_nL_{2n} cages there are far fewer examples of substrate activation. A notable exception is the work of Lusby and colleagues, who have extensively explored Pd_2L_4 cages to bind electrophilic reactants and electronically activate them for attack by a nucleophile[55]. In their earliest example of this work, cage Pd_2**L9**$_4$ was effective in encapsulating a dienophile such as benzoquinone **13**, enhancing its reactivity via hydrogen bonding to the interior pyridine protons (Fig. 4a)[56]. Consequently, the rate of a Diels–Alder cyclization is increased by up to three orders of magnitude compared to the bulk solution. Crucially, co-binding of the diene **14** is not required; the increased reactivity is entirely due to transition-state stabilization provided by favourable hydrogen bonding with the cage protons. Comparatively weak binding of the Diels–Alder product **15** allows for efficient turnover, highlighting a key advantage over previous co-encapsulation strategies, such as the Rebek softball capsules[45], which show substantial product inhibition. In a similar manner, a Michael addition reaction may be catalysed by an M_2L_4 cage by electronic activation of pro-nucleophiles, leading to their enhanced deprotonation, even under base-free conditions[57]. This example demonstrates the power of precise substrate activation to facilitate reactivity even under extremely mild conditions, emulating biological catalysis environments.

An additional feature of small metal–organic cages with defined cavities is the difference in steric and electronic environments at the internal and external faces of the metal node. This characteristic has been exploited by Lusby and colleagues, who used an externally bound substrate at the outside of a metal node to modulate the reactivity of a reactant inside the cage[58]. The externally bound substrate can be considered as an effector or cofactor for the catalyst. Similarly, an internally bound effector has been used by Reek and colleagues to dramatically change the reactivity of an external reactant[59]. This use of effector binding at a secondary site to influence the catalytic rate is reminiscent, albeit to a much simpler degree, of allosteric modulation of enzymatic transformations.

Yang and colleagues have applied a different Pd_2L_4 cage to electronically activate a reactant for alkyl halide cleavage (Fig. 4b)[60]. The use of phenazine ligand **L10** generates a conformationally adaptive cavity in Pd_2**L10**$_4$ that can bind several different anionic guests, reporting exceptionally high binding affinities of up to 10^{14} M^{-1} for halogen anions. As such, the cage could be used to promote the cleavage of carbon–halogen bonds in tertiary halides, in a similar manner to previously reported supramolecular structures with defined cavities[61,62]. Bond scission of alkyl bromide substrate **16** to generate carbocation **17** occurred almost immediately in the presence of Pd_2**L10**$_4$. The conversion of related alkyl chloride reactants was more sluggish, but could be enhanced under UV radiation, exploiting the photoredox behaviour of ligand **L10**. In contrast, no conversion of **16** was observed when ligand **L10** was used in isolation, either with or without irradiation, highlighting the requirement for the cage cavity to activate the carbon–bromine bond and stabilize the resulting anion. The racemization of an enantiomerically pure alkyl halide reactant suggested an S_N1 reaction mechanism was favoured for this process. However, the extremely strong halide binding affinity of this system prevents turnover, leading to stochiometric transformations.

As an alternative to binding a reactant within an M_2L_4 cage, a catalyst or cofactor may also be electronically activated by similar means. For example, a [4 + 2] cyclization reaction may be activated by binding quinone cofactor **18** within a cage Pd_2**L11**$_4$, thus enhancing the oxidative properties of **18** and promoting radical–cation cycloaddition reactions in the bulk (Fig. 4c)[63]. The Diels–Alder reaction of **19** and **20** to form **21** proceeds in 99% yield in the presence of **18**⊂Pd_2**L11**$_4$, but does not show any reaction when a competitive alternative guest is also present, confirming that the host–guest complex is indeed responsible for

https://doi.org/10.1038/s44160-024-00606-5

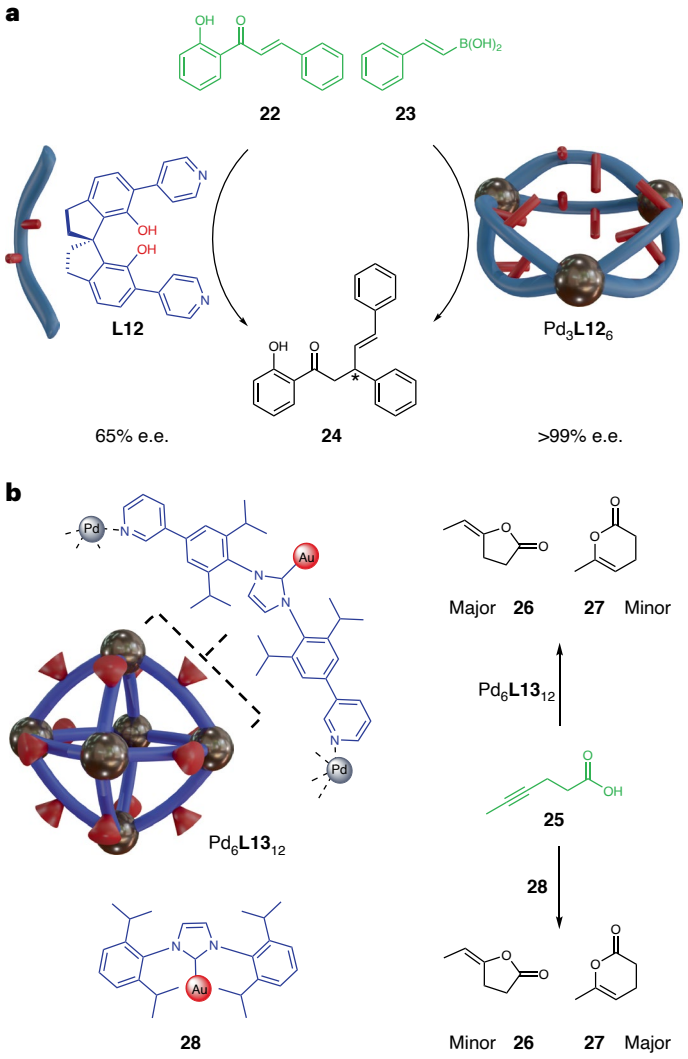

Fig. 5 | M_nL_{2n} cages for reactant preorganization. a, The asymmetric conjugate addition of α,β-enone **22** and styrylboronic acid **23** to yield chiral product **24** is catalysed by ligand **L12**[69]. When **L12** is incorporated into cage Pd_3**L12**$_6$, preorganizing the active hydroxyl catalysts, the e.e. of the reaction is increased from 65% to >99%. **b**, The cyclization of hex-4-ynoic acid **25** is catalysed by *N*-heterocyclic carbene gold complexes, such as ligand **L13** and complex **28**[70]. When **L13** is incorporated into cage Pd_6**L13**$_{12}$, preorganizing reactant **25** in the cage window, five-membered ring **26** is the major product. When catalysed by complex **28**, the six-membered ring **27** is the major product. Ligands are shown in shades of blue, Pd^{2+} nodes as grey spheres, catalysts in red, reactants in green and products in black.

the reactivity. In a further extension of this concept, a photocatalytic host–guest complex activated by the binding of a related extended quinone within a Pd_2L_4 cage is found to catalyse bulk [4 + 2] cycloadditions and aza-Henry reactions[64]. The electronic activation of bound catalysts or cofactors within small metal–organic cages instead of more commonly reported reactants is therefore an elegant alternative for the application of these cages in catalytic transformations, and as the reaction takes place at the rim of the cage rather than inside, product inhibition is not an issue.

Cages for reactant preorganization

For many reactions, the substrate needs to adopt a specific conformation for the reaction to occur, which is typically associated with an entropy penalty. Performing the reaction in a well-defined cavity may lead to preorganization of the substrate in the proper conformation, and as such the binding of the substrate in the cavity reduces the entropy penalty of the reaction. It could be argued that preorganization of a reactant to favour a specific product isomer is simply a specific form of substrate activation. There is a large body of literature highlighting examples of substrate preorganization within tetrahedral M_4L_6 and octahedral M_6L_4 metal–organic cages. For example, the anionic Ga_4L_6 cage of Raymond, Toste and Bergman is known to force a substrate into a conformation preorganized for an aza-Cope rearrangement[65], and invert the stereochemistry of aza-Darzens reactions[66]. Similarly, the octahedral Pd_6L_4 cage of Fujita and colleagues is effective in mechanically twisting amide guests to break their conjugation and therefore enhance their reactivity[67], and is also able to preorganize flexible substrates for otherwise entropically expensive tetradehydro-Diels–Alder reactions[68]. The scope of tetrahedral and octahedral metal–organic cages to preorganize various different substrates for distinct reactions is probably a result of their cavity size—perfect for tightly encapsulating individual small molecules and cyclic transition states. This breadth of examples is not mirrored in the M_2L_4 cage literature, possibly because these cavities tend to be too small for significant substrate preorganization. In addition, the narrow ligands incorporated in most M_2L_4 cages lead to large portals at the cage windows, providing less steric hindrance to force bound guests into folded conformations. However, slightly larger iterations of M_nL_{2n} cages do show potential for substrate preorganization. Liu and colleagues have reported a chiral Pd_3L_6 cage composed of 1′-spirobiindane-7,7′-diol-based ligand **L12**, which can catalyse the asymmetric conjugate addition of α,β-enone **22** and styrylboronic acid **23** to yield chiral product **24** (Fig. 5a)[69]. Using cage Pd_3**L12**$_6$ enabled very high enantioselectivities, with a reported enantiomeric excess (e.e.) of **24** of >99%, compared to ligand **L12** alone, which showed a much lower e.e. of ~65%. Using bulky alternative substrates to **22** and **23** led to much slower conversion, suggesting that the reaction occurs primarily within the cage and that the observed enantioselectivity is due to preorganization of the substrates within its restricted chiral microenvironment.

In addition to the interior of cages, the cage windows also present well-defined M_nL_{2n} pockets that may allow substrate preorganization. For example, medium-sized M_6L_{12} cages may have ideal dimensions to preorganize small substrate molecules within the cage windows, rather than the centre of the cavity. Jing, Duan and Reek recently reported a Pd_6L_{12} cage assembled from ligand **L13** functionalized with rigid *N*-heterocyclic carbene gold complexes (Fig. 5b)[70]. Cage Pd_6**L13**$_{12}$ is found to catalyse the cyclization of hex-4-ynoic acid **25**. Preorganization of **25** at the rigid windows of cage Pd_6**L13**$_{12}$ is effective in modulating the reaction selectivity. When the reaction is catalysed within the confined space of the cage window, **25** preferentially forms five-membered ring **26** over six-membered regioisomer **27**, showing a **26**:**27** ratio of 1.2. However, the six-membered product **27** is formed preferentially in the presence of alternative *N*-heterocyclic carbene gold complex **28**, showing a **26**:**27** ratio of 0.7. This switching of product regioselectivity is the direct result of substrate preorganization, in which the sterically restricted cage window favours the smaller intramolecular reaction.

Cages demonstrating multiple roles

The examples throughout this Review have been selected to highlight specific roles of the relevant M_nL_{2n} cages in specific reactions that they catalyse, such as catalyst concentration or isolation and substrate preorganization. However, a cage may perform multiple different roles, as some features can be interconnected. Although the utility of M_nL_{2n} cages and related structures[71] for different, yet associated, roles may initially have developed serendipitously, multifaceted roles of a single cage in catalysis can be deliberately targeted by rational design.

In one example where a cage performs multiple roles, Reek and colleagues reported a $Pt_{12}L_{24}$ cage functionalized with hydrogen-bond donors that are able to co-encapsulate multiple different components, simultaneously enhancing the concentration of the catalyst and the

https://doi.org/10.1038/s44160-024-00606-5

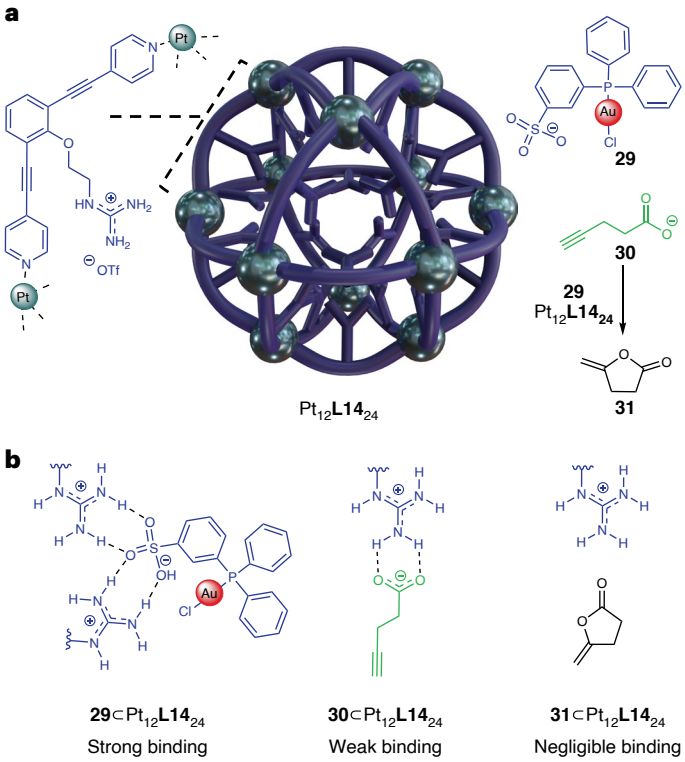

Fig. 6 | The different roles of a $Pt_{12}L_{24}$ cage with respect to different substrates. a, Nanosphere Pt_{12}**L14**$_{24}$ accelerates the cyclization of acetylenic acid **30** to its enol lactone product **31**, which is catalysed by Au(I) catalyst **29**. **b**, The sulfonate group on Au(I) catalyst **29** binds much more strongly to the guanidinum moieties of Pt_{12}**L14**$_{24}$ than the carboxylate group of reactant **30**, and the binding of product **31** is negligible, ensuring efficient catalytic turnover. The role of cage Pt_{12}**L14**$_{24}$ is therefore to enhance the concentration of **29** throughout the reaction, but to preorganize **30** in place only transiently. Ligands are shown in shades of blue, Pt^{2+} nodes as turquoise spheres, catalysts in red, reactants in green and products in black[72].

reactant, and at the same time leading to preorganization of the respective components (Fig. 6)[72]. Ligand **L14**, featuring an endohedral guanidinium moiety, was incorporated into nanosphere Pt_{12}**L14**$_{24}$ (Fig. 6a). Au(I) catalyst **29** was effective in catalysing the cyclization of acetylenic acid **30** to its enol lactone product **31**. A tenfold increase in cyclization rate is reported in the presence of cage Pt_{12}**L14**$_{24}$, compared to the free ligand **L14**. By design, the cage has a different affinity for catalyst **29** and reactant **30**. The sulfonate group of **29** interacts with the guanidium moieties of **L14** in a 1:1 ratio, resulting in a binding strength of 330 M^{-1}, whereas the binding of **29** with Pt_{12}**L14**$_{24}$ displays a binding constant of >10^5 M^{-1}, in line with stronger multitopic binding of sulfonate groups (Fig. 6b). In contrast, reactant **30** bears a carboxylate group allowing only monotopic binding, leading to weaker binding (1,849 M^{-1}), and as a result the substrate can be present in excess with respect to the catalyst without displacing it from the cage. The negligible binding of product **31** facilitates efficient turnover of the cyclization reaction without compromising the enhanced concentration of either reactant or catalyst within cage Pt_{12}**L14**$_{24}$ (Fig. 6b). Because both catalyst and reactant interact with the same guanidinium tethers within the nanosphere, the intermolecular distance between the two is also optimized for precise organization of **30** with respect to the Au(I) catalyst **29**, leading to selectivity in the cyclization. In subsequent work concerning more challenging alkynoic acid reactants with internal acetylene groups, the cyclization reaction regioselectivity was also influenced by the local concentration of gold catalyst, which was easily adjusted by just mixing the gold catalyst and the nanosphere in different ratios[73]. By increasing the catalytic complexity towards multicomponent substrate preorganization, these cage architectures begin to emulate the sophistication of enzymatic catalytic triads[74].

The role of the cage can also change while the reaction is progressing. An example of this concept was reported by Fujita and colleagues in the context of controlling guest polymerization (Fig. 7)[75]. A $Pd_{12}L_{24}$ cage with a cationic interior was generated by the incorporation of an endohedral ammonium functionality within ligand **L15** (Fig. 7a). Nanosphere Pd_{12}**L15**$_{24}$ binds anionic sodium *p*-styrenesulphonate monomers **32**. Following redox initiation with a mixture of $(NH_4)_2S_2O_8$ and $NaHSO_3$, which also binds within the cage, **32** polymerizes to yield product **33**. The role of Pd_{12}**L15**$_{24}$ changes over the course of the reaction (Fig. 7b). The cationic nanosphere first enhances the local concentration of anionic monomer **32**, thus increasing the initial rate of polymerization more than fourfold upon redox initiation when compared to the bulk reaction. This increase in initial rate is probably also due to spatial preorganization of the monomers close to each other and to the initiator, because of the precise spacing of the templating cationic groups within the nanosphere. The number-average molecular weight of the obtained polymer **33** was 2,860 in the presence of cage Pd_{12}**L15**$_{24}$, compared to 5,800 in the bulk solution, and the polydispersity indices of the two were 1.61 and 3.53, respectively. Once the polymerization reaction has proceeded to a certain degree, the nanosphere Pd_{12}**L15**$_{24}$ restricts the polymerized product **33** from further reaction and the polyanion/polycation complex precipitates. As a result, the encapsulated polymer

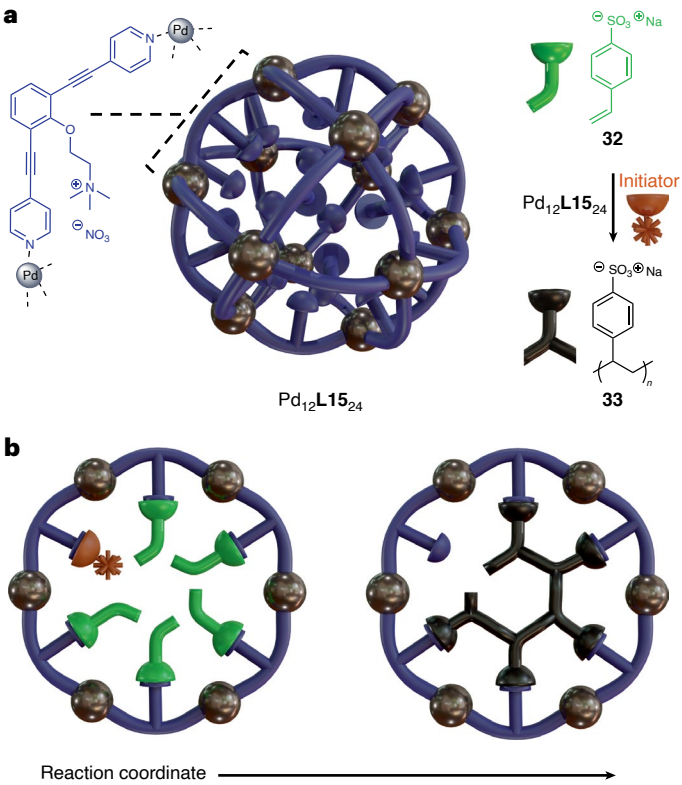

Fig. 7 | The changing role of a $Pd_{12}L_{24}$ cage over the course of a reaction. a, Styrene monomer **32** is encapsulated within nanosphere Pd_{12}**L15**$_{24}$ by favourable ionic interactions between the sulfonate groups of **32** and the ammonium groups of **L15**. Upon redox initiation, polymerization of **32** to **33** occurs within the cage. **b**, A cross-sectional view of cage Pd_{12}**L15**$_{24}$ highlights its changing role over the course of the reaction. First, the binding of multiple monomers **32** close in space increases their local concentration and preorganizes them for polymerization. After the resulting polymer **33** reaches a certain size, cage Pd_{12}**L15**$_{24}$ protects it from further polymerization by both steric repulsion and reduced solubility due to charge accumulation. Ligands are shown in shades of blue, Pd^{2+} nodes as grey spheres, redox initiator in orange, reactants in green and products in black[75].

https://doi.org/10.1038/s44160-024-00606-5

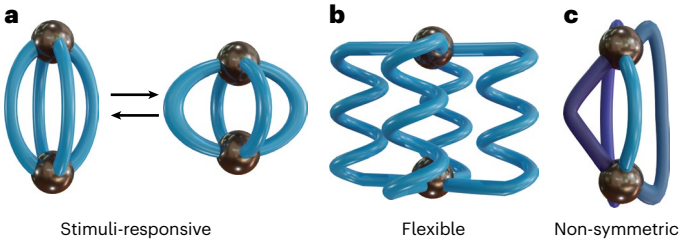

Fig. 8 | Increasing structural complexity in M_nL_{2n} cages. a, Stimuli-responsive cages can change their size or composition under an external stimulus such as light irradiation or guest addition. **b**, Cages incorporating flexible ligands have the potential for adaptive binding in response to varied guests. **c**, Non-symmetric cages provide a means of achieving cavity anisotropy. Ligands are shown in shades of blue and Pd^{2+} nodes as grey spheres.

is protected at a specific molecular weight and thus the polydispersity can be controlled. Non-covalent binding between the cage template and the reactant potentially allows for straightforward expansion of this strategy to different reactions and substrates.

Outlook

In past decades the catalytic toolbox for organic chemists has gradually grown, and today, most total synthesis protocols include steps that involve a metal-catalysed step, typically leading to shorter and more sustainable synthetic routes. The use of cages in organic transformations has so far been mostly the domain of supramolecular chemistry and has largely been explorative. However, we have now reached a state where the application of cages in synthesis can also be considered by organic chemists without experience in supramolecular chemistry. To be widely embraced as feasible components in catalysed reactions, it is vital that M_nL_{2n} cages be readily available or very easily synthesized. Indeed, the simplistic nature of the constituent ligands has already led to the commercial availability of some dipyridyl building blocks, thus requiring only complexation with the appropriate metal node to form the active cage species[76,77]. Lowering the synthetic barrier in this manner is vital to allow chemists with no supramolecular expertise or interest to also benefit from the potential of M_nL_{2n} cages in catalysis.

M_nL_{2n} cages can be utilized to solve a variety of issues by fulfilling different specific roles. Cages can be used as molecular flasks by controlling the concentration of substrates[13]. They can also impose reactivity on encapsulated substrates, as the environment within the cage can be different compared to the bulk, and as such they operate as real catalysts. In addition, cages can also be considered as 'molecular moulds' for the preorganization of a substrate, leading to either faster reactions or selective reactions. Also, cages can protect substrates or, more importantly, catalysts from harsh reaction conditions or from complementary catalysts that are used for tandem catalysis. Further specific roles of M_nL_{2n} cages include the modulation of substrate solubility through host–guest binding, thus enabling catalytic transformations to occur in otherwise incompatible reaction conditions[78]. This has implications for the further expansion of metal–organic cages for in vivo use, in which the requirement for aqueous solubility limits traditional transition-metal catalysis. Translating the application of metal–organic cages from the aqueous phase to biologically relevant reaction media is not trivial because of the presence of coordinating salts and biomolecules that can decompose the structure[79], but initial reports have demonstrated that the compatibility issues can be solved[33,80,81]. Consideration of the application of cage architectures in different complementary roles from multiple synthetic angles will enable further development of the synthetic toolbox. Ultimately, this multifaceted approach may enable complex catalytic reactions and enzyme-like transformations incorporating allosteric modulation and host–guest-induced feedback loops[58,59]. Considering the transition of feedstock from oil-based to biomass and biogenic waste in the near future, the application of cages may be a powerful tool to enable selective transformations in more complex media.

In addition to further exploration of potential applications of cages in synthesis, the cage catalysis field should also further develop, for example by increasing structural complexity. Incorporating stimuli-responsive elements in cages can induce substantial changes in their properties—and therefore their role—in situ (Fig. 8a). For example, the photoisomerization of ligand components has led to the development of M_nL_{2n}[82] and related[83] cages that undergo significant structural changes under light irradiation. Binding of a different guest molecule, or modification of a guest in situ, may also induce a change in the cage architecture[84]. By modifying the size[85] or composition[86] of an M_nL_{2n} cage in situ under an external stimulus, the ability to switch a role, such as activation or preorganization, on or off may be attained.

A further means of introducing adaptivity and responsiveness to molecular cages is to increase their flexibility (Fig. 8b). In general, metal–organic cages are almost exclusively derived from rigid ligands, leading to the predictable and reliable formation of supramolecular structures with defined size and shape. This approach is strikingly different to the 'induced fit' approach of flexible biological hosts, which can adapt to the shape of their guest, and can lead to substantial catalytic rate acceleration[87]. Flexible cage structures have the potential for adaptive activation and preorganization within a complex reaction mixture. In a recent example of flexible M_nL_{2n} cages, McTernan and colleagues have reported a novel class of easily scalable metal–peptidic cages that can bind various biologically relevant guests, such as amino acids and therapeutic molecules[88]. Future exploration of such cages and related structures is likely to have significant application in a catalytic context[89]. Closely related to flexibility is the exploration of the effects of dynamic structural changes that occur between steps in the catalytic cycle, as is now widely recognized in the context of conformational dynamics in enzyme catalysis[90]. Conformational dynamics of the cage structure on the reaction timescale may facilitate increased rates and selectivities of specific catalytic steps, and thus result in emergent phenomena[91,92].

Recent developments in heteroleptic and low-symmetry cage synthesis also offer new opportunities for constructing multifunctional catalysts[93]. Although a key advantage of M_nL_{2n} cages is their modularity and simplicity of structure, this can limit the complexity of their potential functions, especially compared to their biological counterparts[94]. Indeed, enzyme catalytic sites generally have no symmetry elements at all. Great progress in the targeting of cavity anisotropy has been reported in recent years by Clever[95], Crowley[96], Preston[97] and Lewis[98], among others (Fig. 8c). Although primarily limited to the simplest M_2L_4 cages at present, the future will probably see comparable strides in the rational design of low-symmetry cages of larger and more complex structure as robust design principles are established[99]. Controlling the type and position of different ligands may allow the precise placement of functional groups, allowing a means of constructing artificial catalytic triads[74]. Multicompartment cages may also provide a powerful means of expanding cavity complexity[100].

The advent of stimuli-responsive, flexible and non-symmetric structures is thus a crucial step towards further emulating biological structures in enhancing the different roles of M_nL_{2n} cages. Such versatile cage structures have the potential to provide unique reactivity and control over catalysed reactions, suggesting a future with improved spatial and temporal control over catalysis. With important advances in synthesis and application already demonstrated in recent years, it is very possible that metal–organic cages may soon assume a routine role in synthetic chemistry. Although the focus of this Review is M_nL_{2n} systems, such considerations are likely to also be directly applicable to other metal–organic and even purely organic cage architectures. With this Review we have highlighted the multifaceted role of cage catalysts, which should promote the use of these readily accessible, robust and versatile catalysts as an ubiquitous choice for mediating synthetic reactions.

References

1. Lehn, J.-M. Supramolecular chemistry—scope and perspectives: molecules, supermolecules and molecular devices (Nobel Lecture). *Angew. Chem. Int. Ed. Engl.* **27**, 89–112 (1988).
2. Wiester, M. J., Ulmann, P. A. & Mirkin, C. A. Enzyme mimics based upon supramolecular coordination chemistry. *Angew. Chem. Int. Ed.* **50**, 114–137 (2010).
3. Chorkendorff, I. & Niemantsverdriet, J. W. *Concepts of Modern Catalysis and Kinetics* (Wiley, 2007).
4. van Leeuwen, P. W. N. M. & Raynal, M. (eds) *Supramolecular Catalysis: New Directions and Developments* (Wiley, 2022).
5. Gokel, G. W. & Durst, H. D. Principles and synthetic applications in crown ether chemistry. *Synthesis* **1976**, 168–184 (1976).
6. Di Stefano, S., Capocasa, G. & Mandolini, L. Supramolecular catalysts featuring crown ethers as recognition units. *Eur. J. Org. Chem.* **2020**, 3340–3350 (2020).
7. Xue, Y. et al. Catalysis within coordination cages. *Coord. Chem. Rev.* **430**, 213656 (2021).
8. Arnold, F. H. Directed evolution: bringing new chemistry to life. *Angew. Chem. Int. Ed.* **57**, 4143–4148 (2017).
9. Pilgrim, B. S. & Champness, N. R. Metal–organic frameworks and metal–organic cages—a perspective. *ChemPlusChem* **85**, 1842–1856 (2020).
10. Piskorz, T. K., Martí-Centelles, V., Spicer, R. L., Duarte, F. & Lusby, P. J. Picking the lock of coordination cage catalysis. *Chem. Sci.* **14**, 11300–11331 (2023).
11. Grommet, A. B., Feller, M. & Klajn, R. Chemical reactivity under nanoconfinement. *Nat. Nanotechnol.* **15**, 256–271 (2020).
12. Leenders, S. H. A. M., Gramage-Doria, R., de Bruin, B. & Reek, J. N. H. Transition metal catalysis in confined spaces. *Chem. Soc. Rev.* **44**, 433–448 (2015).
13. Yoshizawa, M., Klosterman, J. K. & Fujita, M. Functional molecular flasks: new properties and reactions within discrete, self-assembled hosts. *Angew. Chem. Int. Ed.* **48**, 3418–3438 (2009).
14. Harris, K., Fujita, D. & Fujita, M. Giant hollow M_nL_{2n} spherical complexes: structure, functionalisation and applications. *Chem. Commun.* **49**, 6703–6712 (2013).
15. Han, M., Engelhard, D. M. & Clever, G. H. Self-assembled coordination cages based on banana-shaped ligands. *Chem. Soc. Rev.* **43**, 1848–1860 (2014).
16. Tarzia, A., Wolpert, E. H., Jelfs, K. E. & Pavan, G. M. Systematic exploration of accessible topologies of cage molecules via minimalistic models. *Chem. Sci.* **14**, 12506–12517 (2023).
17. Liao, P. et al. Two-component control of guest binding in a self-assembled cage molecule. *Chem. Commun.* **46**, 4932–4934 (2010).
18. Schmidt, A., Casini, A. & Kühn, F. E. Self-assembled M_2L_4 coordination cages: synthesis and potential applications. *Coord. Chem. Rev.* **275**, 19–36 (2014).
19. McMorran, D. A. & Steel, P. J. The first coordinatively saturated, quadruply stranded helicate and its encapsulation of a hexafluorophosphate anion. *Angew. Chem. Int. Ed.* **37**, 3295–3297 (1998).
20. August, D. P., Nichol, G. S. & Lusby, P. J. Maximizing coordination capsule–guest polar interactions in apolar solvents reveals significant binding. *Angew. Chem. Int. Ed.* **55**, 15022–15026 (2016).
21. Rota Martir, D. et al. A Pd_3L_6 supramolecular cage incorporating photoactive [2.2]paracyclophane units. *Inorg. Chem. Front.* **7**, 232–238 (2020).
22. Wu, M.-X. et al. Self-assembly of conformation-adaptive dihydrophenazine-based coordination cages. *Chem. Commun.* **60**, 1184–1187 (2024).
23. Mesquita, L. M. et al. Palladium(II)-mediated assembly of a M_2L_2 macrocycle and M_3L_6 cage from a cyclopeptide-derived ligand. *Org. Lett.* **21**, 6442–6446 (2019).
24. Chand, D. K. et al. Dynamic self-assembly of an M_3L_6 molecular triangle and an M_4L_8 tetrahedron from naked Pd^{II} ions and bis(3-pyridyl)-substituted arenes. *Chem. Asian J.* **1**, 82–90 (2006).
25. Tateishi, T., Kojima, T. & Hiraoka, S. Multiple pathways in the self-assembly process of a Pd_4L_8 coordination tetrahedron. *Inorg. Chem.* **57**, 2686–2694 (2018).
26. Li, R.-J., Marcus, A., Fadaei-Tirani, F. & Severin, K. Orientational self-sorting: formation of structurally defined Pd_4L_8 and Pd_6L_{12} cages from low-symmetry dipyridyl ligands. *Chem. Commun.* **57**, 10023–10026 (2021).
27. Frank, M., Johnstone, M. D. & Clever, G. H. Interpenetrated cage structures. *Chem. Eur. J.* **22**, 14104–14125 (2016).
28. Suzuki, K., Tominaga, M., Kawano, M. & Fujita, M. Self-assembly of an M_6L_{12} coordination cube. *Chem. Commun.* **2009**, 1638–1640 (2009).
29. Tominaga, M. et al. Finite, spherical coordination networks that self-organize from 36 small components. *Angew. Chem. Int. Ed.* **43**, 5621–5625 (2004).
30. Fujita, D. et al. Protein encapsulation within synthetic molecular hosts. *Nat. Commun.* **3**, 1093 (2012).
31. Sun, Q.-F. et al. Self-assembled $M_{24}L_{48}$ polyhedra and their sharp structural switch upon subtle ligand variation. *Science* **328**, 1144–1147 (2010).
32. Yoneya, M., Tsuzuki, S., Yamaguchi, T., Sato, S. & Fujita, M. Coordination-directed self-assembly of $M_{12}L_{24}$ nanocage: effects of kinetic trapping on the assembly process. *ACS Nano* **8**, 1290–1296 (2014).
33. Bobylev, E. O., Poole, D. A., de Bruin, B. & Reek, J. N. H. How to prepare kinetically stable self-assembled $Pt_{12}L_{24}$ nanocages while circumventing kinetic traps. *Chem. Eur. J.* **27**, 12667–12674 (2021).
34. Otte, M. Reactions in endohedral functionalized cages. *Eur. J. Org. Chem.* **26**, e202300012 (2023).
35. Cram, D. J., Tanner, M. E. & Thomas, R. The taming of cyclobutadiene. *Angew. Chem. Int. Ed. Engl.* **30**, 1024–1027 (1991).
36. Li, Y. & Houk, K. N. The dimerization of cyclobutadiene. An ab initio CASSCF theoretical study. *J. Am. Chem. Soc.* **118**, 880–885 (1996).
37. Ueda, Y., Ito, H., Fujita, D. & Fujita, M. Permeable self-assembled molecular containers for catalyst isolation enabling two-step cascade reactions. *J. Am. Chem. Soc.* **139**, 6090–6093 (2017).
38. Brown, C. M. et al. Endohedrally functionalized metal-organic cage-cross-linked polymer gels as modular heterogeneous catalysts. *J. Am. Chem. Soc.* **144**, 13276–13284 (2022).
39. Zhu, F.-F. et al. Confinement self-assembly of metal-organic cages within mesoporous carbon for one-pot sequential reactions. *Chem* **6**, 2395–2406 (2020).
40. Moad, G. & Solomon, D. H. *The Chemistry of Radical Polymerization* (Elsevier, 2006).
41. Yamashina, M., Sei, Y., Akita, M. & Yoshizawa, M. Safe storage of radical initiators within a polyaromatic nanocapsule. *Nat. Commun.* **5**, 4662 (2014).
42. Mal, P., Breiner, B., Rissanen, K. & Nitschke, J. R. White phosphorus is air-stable within a self-assembled tetrahedral capsule. *Science* **324**, 1697–1699 (2009).
43. Pullen, S., Löffler, S., Platzek, A., Holstein, J. J. & Clever, G. H. Substrate and product binding inside a stimuli-responsive coordination cage acting as a singlet oxygen photosensitizer. *Dalton Trans.* **49**, 9404–9410 (2020).
44. Fujita, D. et al. Protein stabilization and refolding in a gigantic self-assembled cage. *Chem* **7**, 2672–2683 (2021).
45. Kang, J. & Rebek, J. Acceleration of a Diels–Alder reaction by a self-assembled molecular capsule. *Nature* **385**, 50–52 (1997).
46. Sanders, J. K. M. Supramolecular catalysis in transition. *Chem. Eur. J.* **4**, 273–286 (1999).

47. Gramage-Doria, R. et al. Gold(I) catalysis at extreme concentrations inside self-assembled nanospheres. *Angew. Chem. Int. Ed.* **53**, 13380–13384 (2014).
48. Leenders, S. H. A. M., Dürr, M., Ivanović-Burmazović, I. & Reek, J. N. H. Gold functionalized platinum $M_{12}L_{24}$-nanospheres and their application in cyclization reactions. *Adv. Synth. Catal.* **358**, 1509–1518 (2016).
49. Gonell, S., Caumes, X., Orth, N., Ivanović-Burmazović, I. & Reek, J. N. H. Self-assembled $M_{12}L_{24}$ nanospheres as a reaction vessel to facilitate a dinuclear Cu(I) catalyzed cyclization reaction. *Chem. Sci.* **10**, 1316–1321 (2019).
50. Yu, F. et al. Control over electrochemical water oxidation catalysis by preorganization of molecular ruthenium catalysts in self-assembled nanospheres. *Angew. Chem. Int. Ed.* **57**, 11247–11251 (2018).
51. Zaffaroni, R., Orth, N., Ivanović-Burmazović, I. & Reek, J. N. H. Hydrogenase mimics in $M_{12}L_{24}$ nanospheres to control overpotential and activity in proton-reduction catalysis. *Angew. Chem. Int. Ed.* **59**, 18485–18489 (2020).
52. Lubitz, W., Ogata, H., Rüdiger, O. & Reijerse, E. Hydrogenases. *Chem. Rev.* **114**, 4081–4148 (2014).
53. Bolliger, J. L., Belenguer, A. M. & Nitschke, J. R. Enantiopure water-soluble $[Fe_4L_6]$ cages: host–guest chemistry and catalytic activity. *Angew. Chem. Int. Ed.* **52**, 7958–7962 (2013).
54. Pluth, M. D., Bergman, R. G. & Raymond, K. N. Acid catalysis in basic solution: a supramolecular host promotes orthoformate hydrolysis. *Science* **316**, 85–88 (2007).
55. Young, T. A., Martí-Centelles, V., Wang, J., Lusby, P. J. & Duarte, F. Rationalizing the activity of an 'artificial Diels–Alderase': establishing efficient and accurate protocols for calculating supramolecular catalysis. *J. Am. Chem. Soc.* **142**, 1300–1310 (2019).
56. Martí-Centelles, V., Lawrence, A. L. & Lusby, P. J. High activity and efficient turnover by a simple, self-assembled 'artificial Diels–Alderase'. *J. Am. Chem. Soc.* **140**, 2862–2868 (2018).
57. Wang, J., Young, T. A., Duarte, F. & Lusby, P. J. Synergistic noncovalent catalysis facilitates base-free Michael addition. *J. Am. Chem. Soc.* **142**, 17743–17750 (2020).
58. Martí-Centelles, V., Spicer, R. L. & Lusby, P. J. Non-covalent allosteric regulation of capsule catalysis. *Chem. Sci.* **11**, 3236–3240 (2020).
59. Bobylev, E. O. et al. Effector regulated catalytic cyclization of alkynoic acids using Pt_2L_4 cages. *Angew. Chem. Int. Ed.* **62**, e202218162 (2023).
60. Jiang, W.-L., Huang, B., Zhao, X.-L., Shi, X. & Yang, H.-B. Strong halide anion binding within the cavity of a conformation-adaptive phenazine-based Pd_2L_4 cage. *Chem* **9**, 2655–2668 (2023).
61. Marcos, V. et al. Allosteric initiation and regulation of catalysis with a molecular knot. *Science* **352**, 1555–1559 (2016).
62. Prakasam, T. et al. Metal-organic self-assembled trefoil knots for C–Br bond activation. *ACS Catal* **9**, 1907–1914 (2019).
63. Spicer, R. L. et al. Host–guest-induced electron transfer triggers radical-cation catalysis. *J. Am. Chem. Soc.* **142**, 2134–2139 (2020).
64. Spicer, R. L. et al. *Exo*-cage catalysis and initiation derived from photo-activating host–guest encapsulation. *Chem. Sci.* **14**, 14140–14145 (2023).
65. Fiedler, D., Bergman, R. G. & Raymond, K. N. Supramolecular catalysis of a unimolecular transformation: aza-Cope rearrangement within a self-assembled host. *Angew. Chem. Int. Ed.* **43**, 6748–6751 (2004).
66. Bierschenk, S. M., Bergman, R. G., Raymond, K. N. & Toste, F. D. A nanovessel-catalyzed three-component aza-Darzens reaction. *J. Am. Chem. Soc.* **142**, 733–737 (2020).
67. Takezawa, H., Shitozawa, K. & Fujita, M. Enhanced reactivity of twisted amides inside a molecular cage. *Nat. Chem.* **12**, 574–578 (2020).
68. Genov, G. R., Takezawa, H., Hayakawa, H. & Fujita, M. Tetradehydro-Diels–Alder reactions of flexible arylalkynes via folding inside a molecular cage. *J. Am. Chem. Soc.* **145**, 17013–17017 (2023).
69. Chu, D. et al. Boosting enantioselectivity of chiral molecular catalysts with supramolecular metal-organic cages. *CCS Chem.* **4**, 1180–1189 (2022).
70. Xu, M. et al. Broadening the catalytic region from the cavity to windows by M_6L_{12} nanospheres in cyclizations. *Chem. Sci.* **14**, 11699–11707 (2023).
71. Jin, Y. et al. Coordination-driven self-assembly of anthraquinone-based metal-organic cages for photocatalytic selective [2+2] cycloaddition. *Dalton Trans.* **50**, 8533–8539 (2021).
72. Wang, Q.-Q. et al. Self-assembled nanospheres with multiple endohedral binding sites pre-organize catalysts and substrates for highly efficient reactions. *Nat. Chem.* **8**, 225–230 (2016).
73. Gonell, S. & Reek, J. N. H. Gold-catalyzed cycloisomerization reactions within guanidinium $M_{12}L_{24}$ nanospheres: the effect of local concentrations. *ChemCatChem* **11**, 1458–1464 (2019).
74. Carter, P. & Wells, J. A. Dissecting the catalytic triad of a serine protease. *Nature* **332**, 564–568 (1988).
75. Kikuchi, T., Murase, T., Sato, S. & Fujita, M. Polymerisation of an anionic monomer in a self-assembled $M_{12}L_{24}$ coordination sphere with cationic interior. *Supramol. Chem.* **20**, 81–94 (2008).
76. Sudan, S. et al. $LiBF_4$-induced rearrangement and desymmetrization of a palladium-ligand assembly. *Angew. Chem. Int. Ed.* **61**, e202201823 (2022).
77. Johnson, A. M. et al. Synthesis and properties of metal–ligand complexes with endohedral amine functionality. *Inorg. Chem.* **50**, 9430–9442 (2011).
78. Bobylev, E. O., Poole, D. A., de Bruin, B. & Reek, J. N. H. M_6L_{12} nanospheres with multiple C_{70} binding sites for $^1O_2$ formation in organic and aqueous media. *J. Am. Chem. Soc.* **144**, 15633–15642 (2022).
79. James, C. C., de Bruin, B. & Reek, J. N. H. Transition metal catalysis in living cells: progress, challenges and novel supramolecular solutions. *Angew. Chem. Int. Ed.* **62**, e202306645 (2023).
80. Bobylev, E. O. et al. In vivo biodistribution of kinetically stable Pt_2L_4 nanospheres that show anti-cancer activity. *Chem. Sci.* **14**, 6943–6952 (2023).
81. Bobylev, E. O. et al. The application of $M_{12}L_{24}$ nanocages as cell-specific siRNA delivery agents in vitro. *Chem* **9**, 1578–1593 (2023).
82. Benchimol, E., Tessarolo, J. & Clever, G. H. Photoswitchable coordination cages. *Nat. Chem.* **16**, 13–21 (2024).
83. Oldknow, S. et al. Structure-switching M_3L_2 Ir(III) coordination cages with photo-isomerising azo-aromatic linkers. *Chem. Sci.* **9**, 8150–8159 (2018).
84. Percástegui, E. G. Guest-induced transformations in metal–organic cages. *Eur. J. Inorg. Chem.* **2021**, 4425–4438 (2021).
85. Li, R.-J., Holstein, J. J., Hiller, W. G., Andréasson, J. & Clever, G. H. Mechanistic interplay between light switching and guest binding in photochromic [Pd_2dithienylethene$_4$] coordination cages. *J. Am. Chem. Soc.* **141**, 2097–2103 (2019).
86. Kennedy, A. D. W., DiNardi, R. G., Fillbrook, L. L., Donald, W. A. & Beves, J. E. Visible-light switching of metallosupramolecular assemblies. *Chem. Eur. J.* **28**, e202104461 (2022).
87. Jarvo, E. R., Copeland, G. T., Papaioannou, N., Bonitatebus, P. J. & Miller, S. J. A biomimetic approach to asymmetric acyl transfer catalysis. *J. Am. Chem. Soc.* **121**, 11638–11643 (1999).
88. Barber, B. E, Jamieson, E. M. G., White, L. E. M. & McTernan, C. T. Metal-peptidic cages—helical oligoprolines generate highly anisotropic nanospaces with emergent isomer control. *Chem* https://doi.org/10.1016/j.chempr.2024.05.002 (2024).
89. Sawada, T. et al. Metal–peptide rings form highly entangled topologically inequivalent frameworks with the same ring- and crossing-numbers. *Nat. Commun.* **10**, 921 (2019).

90. Henzler-Wildman, K. & Kern, D. Dynamic personalities of proteins. *Nature* **450**, 964–972 (2007).
91. Gallagher, J. M., Roberts, B. M. W., Borsley, S. & Leigh, D. A. Conformational selection accelerates catalysis by an organocatalytic molecular motor. *Chem* **10**, 855–866 (2024).
92. Liu, W. & Stoddart, J. F. Emergent behavior in nanoconfined molecular containers. *Chem* **7**, 919–947 (2021).
93. Pullen, S. & Clever, G. H. Mixed-ligand metal–organic frameworks and heteroleptic coordination cages as multifunctional scaffolds—a comparison. *Acc. Chem. Res.* **51**, 3052–3064 (2018).
94. Lewis, J. E. M. Developing sophisticated microenvironments in metal-organic cages. *Trends Chem.* **5**, 717–719 (2023).
95. Wu, K., Benchimol, E., Baksi, A. & Clever, G. H. Non-statistical assembly of multicomponent [Pd2ABCD] cages. *Nat. Chem* **16**, 584–591 (2024).
96. Vasdev, R. A. S. et al. Exploiting supramolecular interactions to control isomer distributions in reduced-symmetry $[Pd_2L_4]^{4+}$ cages. *Inorg. Chem.* **62**, 1833–1844 (2023).
97. Preston, D. & Evans, J. D. A lantern-shaped Pd(II) cage constructed from four different low-symmetry ligands with positional and orientational control: an ancillary pairings approach. *Angew. Chem. Int. Ed.* **62**, e202314378 (2023).
98. Lewis, J. E. M. Pseudo-heterolepticity in low-symmetry metal–organic cages. *Angew. Chem. Int. Ed.* **61**, e202212392 (2022).
99. Tarzia, A., Lewis, J. E. M. & Jelfs, K. E. High-throughput computational evaluation of low symmetry Pd_2L_4 cages to aid in system design. *Angew. Chem. Int. Ed.* **60**, 20879–20887 (2021).
100. Vasdev, R. A. S., Preston, D. & Crowley, J. D. Multicavity metallosupramolecular architectures. *Chem. Asian J.* **12**, 2513–2523 (2017).

Acknowledgements

We thank the University of Amsterdam Research Priority Area in Sustainable Chemistry for funding.

Author contributions

Z.A. and J.N.H.R. contributed to discussions and wrote the manuscript.

Competing interests

The authors declare no competing interests.

Additional information

Correspondence and requests for materials should be addressed to Zoe Ashbridge or Joost N. H. Reek.

Peer review information *Nature Synthesis* thanks the anonymous reviewers for their contribution to the peer review of this work. Primary Handling Editor: Alexandra Groves, in collaboration with the *Nature Synthesis* team.